

Pokhrel

Improving the robustness of heat transfer on the floor of naturally ventilated buildings

M. K Pokhrel¹, T. N. Anderson¹ and T. T. Lie¹

¹*School of Engineering, Computer and Mathematical Sciences, Auckland University of Technology, Auckland, New Zealand*

E-mail: timothy.anderson@aut.ac.nz

Abstract

Building Energy Simulation (BES) programs commonly employ a coupled multi-zone thermal and airflow network modelling approach to evaluate the natural ventilation in buildings. However, the robustness of such thermal-airflow models needs greater scrutiny. In particular, the method for determining the indoor-floor surface convective heat transfer coefficient (CHTC).

In an attempt to make an initial investigation on this problem, this work utilized Computational Fluid Dynamics (CFD) for numerically examining the heat transfer and flow-fields in a typical room with a single sided window. While doing this, the convection heat transfer on the indoor floor surface driven by a thermal buoyancy effect established due to a temperature difference between inside surface of the floor and outside ambient was examined. The result showed that the heat transfer behavior of this partly open room was strongly influenced by the Rayleigh number (Ra) and the Window Opening Fraction (WOF). Further, it was found that the heat transfer on the floor varied significantly in a spatial context within the floor. As such, there is a significant scope of increasing the robustness of thermal models of naturally ventilated buildings by greater utilization of empirical relationships developed particularly for this purpose.

1. Introduction

Newton introduced the fundamental concept of Convection Heat Transfer Coefficient (CHTC) through his law of cooling expressed in a general form of equation 1, where the rate of convection heat transfer (q_c) is proportional to the temperature difference between surface and surrounding fluid (Yunus and Afshin, 2015). However, the significant portion of the function is related to identifying CHTC (h_c in equation 1), because it is influenced by various factors mainly – the mechanism of fluid flow, flow regime, properties of the fluid and geometry of the specific system in consideration.

$$q_c = h_c \cdot \Delta T \quad (1)$$

The law is commonly employed in the BES programs to predict the indoor air temperature on the basis of multi-zone thermal model; which in conjunction with airflow network model can also be used to predict airflow through the openings (Hiller et al., 2002) making it useful for

the naturally ventilated building modelling as well. While doing this, it is possible to insert a relevant empirical correlation of CHTC as needed in most of the BES programs to evaluate the heat transfer from building surfaces. As such, it is apparent that the more precise the empirical correlation of the CHTC considered, the resulting building thermal model would be more robust.

In this context, following the coupled thermal and airflow modelling technique, Pokhrel (2016) demonstrated that BES can capture the effect of the natural ventilation through an opening in a model house and illustrated a significant potential for regulating the thermal behavior of relatively airtight and insulated natural ventilated house located in a mild climatic region. However, a sensitivity analysis of various convection correlation by Goethals (2011), Mirsadeghi (2013) and Lomas (1996) demonstrated that the choice of the CHTC correlation strongly affects the energy and thermal comfort predictions. Further to it, Goethals (2011) and Rincón-Casado (2017) also observed that either majority of correlations available in BES are based on isolated horizontal and vertical flat plate surfaces or at most, it is dependent on the temperature difference between opposite surfaces, or surface and zone air. These correlations were developed based on natural convection in the closed enclosure and expressed in terms of Nusselt number (Nu) and Grashof number (Gr) for respective heated surfaces as demonstrated by Awbi and Hatton (1999). Where, the Nu is a non-dimensional number representing convection heat transfer coefficient (Yunus and Afshin, 2015), and is commonly expressed as equation (2), where L_c is the characteristic length and κ is the thermal conductivity of the air obtained at the film-air properties.

$$Nu = h_c \cdot L_c / \kappa \quad (2)$$

Similarly, the Gr is a non-dimensional number representing natural convection effects and expressed as in equation 3, where g is gravitational acceleration, β is volume coefficient of expansion and ν is the kinematic viscosity (Yunus and Afshin, 2015).

$$Gr = g\beta\Delta TL_c^3/\nu^2$$

On the other hand, airflow mechanism in the single sided naturally ventilated buildings is different because of complexity of flow near the opening due to the turbulence created at the opening resulting a pulsation flow (Stabat et al, 2012). As such, the commonly used correlations developed from relatively small (Rincón-Casado et al, 2017 and Corcione, 2003) closed enclosure might be unfit for single sided naturally ventilated building. Despite this, Bilgen and Muftuoglu (2008) computationally examined the flow in an open square cavity with multiple slots and found that the Nu and the volume flow rate both increased with Ra and also the opening ratio. Where Ra is the dimensionless number indicating the natural convection and expressed as a multiplication of Gr and Prandtl Number (Pr) as in equation 4. Whereby, the Pr is another dimensionless number expressed in terms of the ratio of momentum diffusivity ν to the thermal diffusivity (α) as in equation 5.

$$Ra = Gr \cdot Pr \quad (4)$$

$$Pr = \nu / \alpha \quad (5)$$

By utilizing the dimensionless numbers, the average CHTC over a surface is generally expressed as equation (6) in the form of a non-dimensional empirical relationship (Yunus and Afshin, 2015), where constant C and exponent n refers the geometry of the surface and flow regime respectively (n usually falls around 1/4 for laminar and 1/3 for turbulent flow).

$$\text{Nu} = C \cdot \text{Ra}^n \quad (6)$$

Further studies of (Prakash et al, 2012) has delivered an empirical relationship of heat transfer as a function of Ra, opening ratio and inclination for open cavities of different geometries. In yet another series of works of (Norris et al, 2015) and (Anderson et al, 2016), recommended a further three-dimensional numerical studies with wider range of Ra.

Despite the work that has been undertaken, there is still a lack of understanding of the generalised relationships that can be used in determining the heat transfer from the floor in the single-sided naturally ventilated building. As such, this work aims to investigate the problem numerically in three-dimensional domain including only buoyancy driven flow. While doing this, the possible effect due to external wind, transient temperature inside the space, thermal mass of the envelope, solar gains, internal heat loads and furnishings/flow restrictions in the interior spaces were not considered.

2. Methodology

A computational model of a 3D air filled room ($L=2.4$ m, $W=2.4$ m, $H=2.4$ m), was developed in a commercial finite-volume CFD solver available in Fluent software (Figure 1). In performing steady-state simulations the room was placed in a simulation domain with open boundaries a distance $5L$ from the cube external wall upstream, sidewise and top and $15L$ downstream from the rear wall. For the simulations, the floor was assumed to have a temperature of 35°C , while all other walls were assumed to be adiabatic. Three ambient temperature conditions (10°C , 15°C and 20°C) were examined with characteristic length as height of the cube (2.4 m), resulting in $1.9 \times 10^{10} \leq \text{Ra} \leq 3.6 \times 10^{10}$. For this study, a single window ($W=0.9$ m and $H=1.5$ m) was placed in the upstream wall with simulations undertaken assuming Window Opening Fraction (WOF) values 1, 0.75, 0.5 and 0.25.

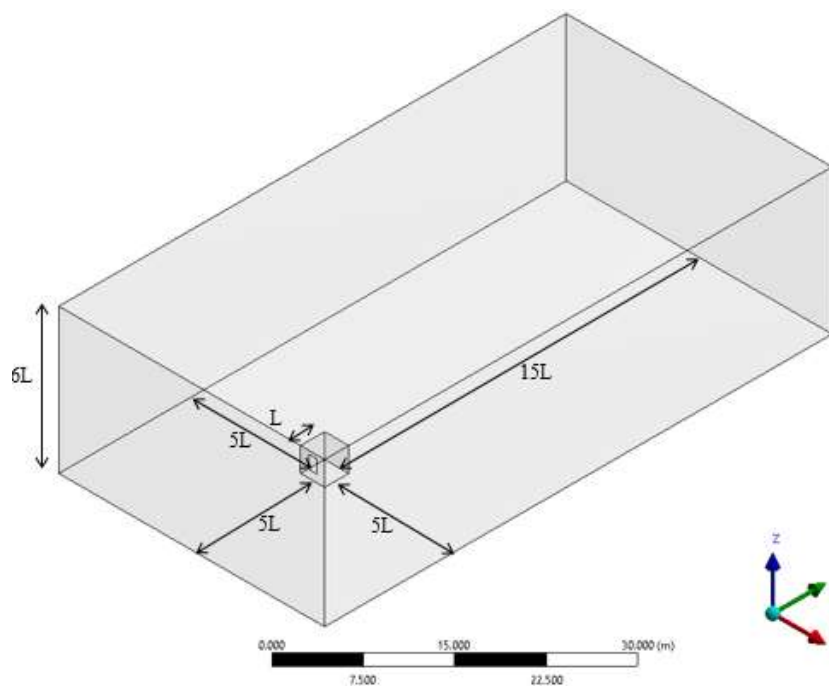


Figure 1. Schematic representation of computational domain and model

An unstructured 3D tetrahedron mesh type with 4.1 million control volumes with inflation layers (first layer height of 0.5 mm and a stretching factor of 1.1) was utilised such that the average y^+ value was significantly less than 1 (~ 0.3), in order to resolve the boundary layer close to the wall. A mesh sensitivity study (Figure 2) was performed before finalizing the number of control volumes to ensure the results to be as mesh independent as possible. While discretization, attention was paid to ensure grid distribution in the boundary layer with several layers in laminar sublayer and buffer layer as described by Omri M. and Galanis N, (2007).

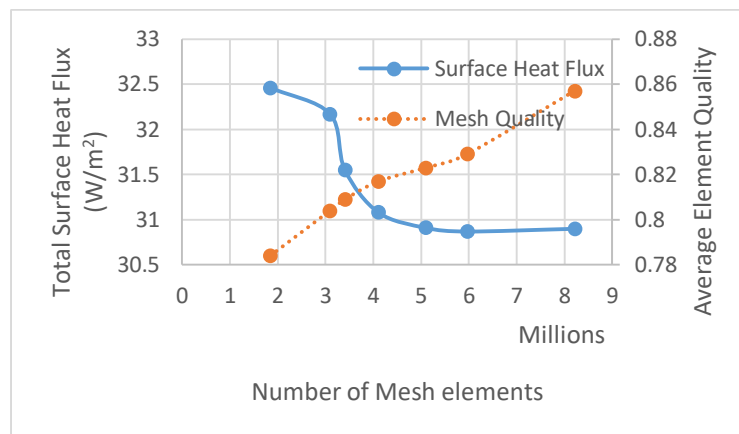


Figure 2. Mesh sensitivity study

The turbulent field was addressed using the $k-\omega$ Shear Stress Transitional (SST) viscous model with the coupling between pressure and velocity distribution resolved using the SIMPLEC scheme. Spatial discretization was performed with the PRESTO pressure scheme and a second order linear upwind difference scheme was employed for the other variables. To demonstrate the 3D behaviour of the mean flow fields at steady state inside the enclosure, post-processing of the computational simulations of all the 12 cases were examined on six different isoplanes as demonstrated in Figure 3.

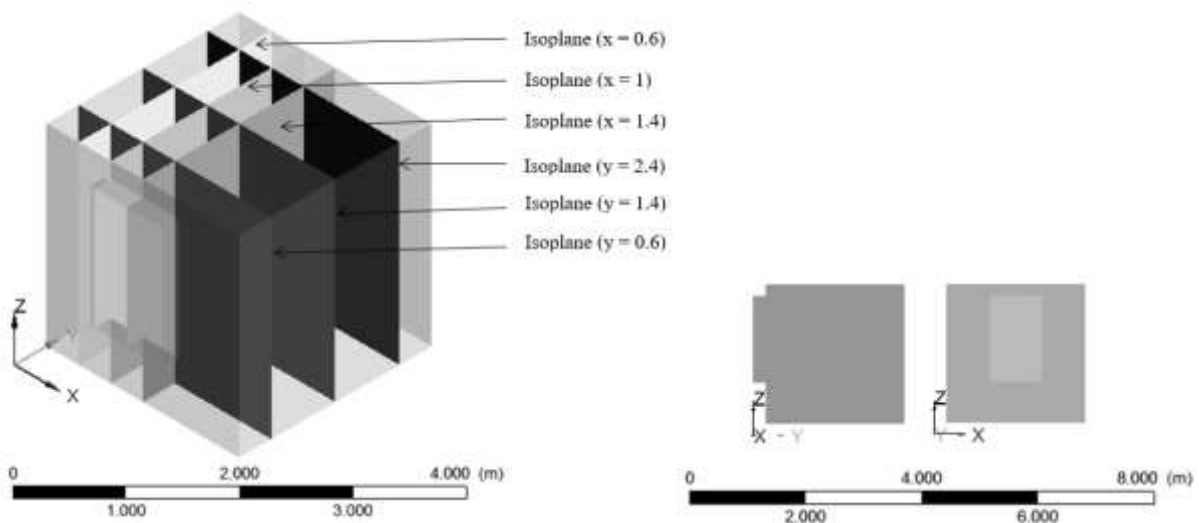


Figure 3. Air filled enclosure (a) Isometric view (b) Front and side views

While doing so, isoplanes ($x=1.4$) and ($y=1.4$) were created on the mid-longitudinal and transverse section of the enclosure respectively. Similarly, additional isoplanes were considered at ($x=0.6$, $y=0.6$ and $y=2.2$) to observe the typical flow fields close (0.4 m) to the vertical walls as shown in Figure 3. Finally, isoplane ($x=1$) which is a longitudinal plane close to the window side edge was selected to observe the flow fields on the cusp of the directly exposed and unexposed region of the opening.

3. Results and Discussion

While examining the flow behaviour on six isoplanes as described in Figure 3, within the threshold of WOF values and Ra number considered, it was identified that the behaviours are similar though the intensity of them was slightly varying in nature. As such, the case with WOF value of 1 and Ra 1.93×10^{10} was selected to demonstrate and discuss a typical three-dimensional flow field behaviour. While doing this, Figure 4 (a) and (b) demonstrates the velocity vector and temperature distribution on isoplane ($x=1.4$).

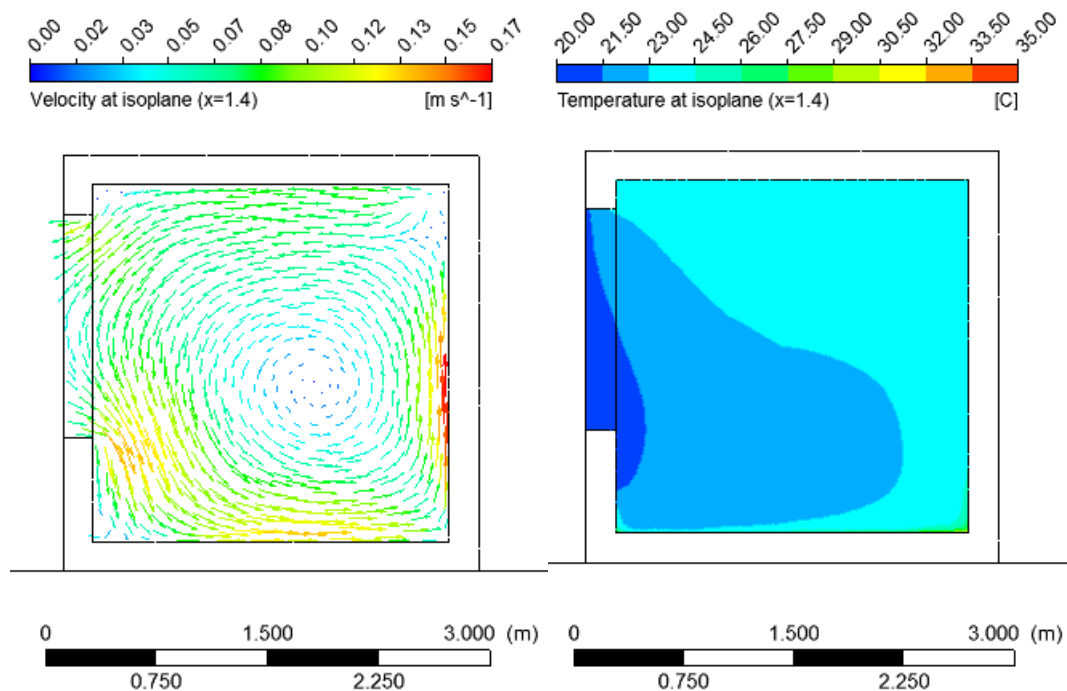


Figure 4. (a) Velocity vector (left) (b) Temperature Contour (right) at isoplane ($x = 1.4$)

It is obvious from the distribution of velocity vector that the flow on this plane as demonstrated in Figure 4(a) is mostly recirculating in nature due to buoyancy effect. However, a significant fresh air plume is drawn to the lower part of the opening from outside the enclosure to maintain continuity as air exits the room due to buoyancy. This contributes significantly to the turbulent flow on the floor adjacent to the window resulting in a higher velocity. Similar to it, observing the temperature distribution on the same plane, Figure 4(b) shows an existence of a varying level of temperature distribution inside the enclosure in the form of increasing its intensity from inlet window towards the opposite wall and from floor to the ceiling of the enclosure. Obviously, this uneven distribution of velocity and temperature, indicate that resulting heat transfer from the floor at the intersection of the plane and floor surface would be relatively non-uniform and weakening in nature as it moves away from the opening.

Furthermore, observing the flow fields on isoplane ($x=1$) as demonstrated in Figure 5(a) for velocity, the recirculating nature observed due to buoyancy effect stays relatively similar throughout the width of the opening. However, the tendency of recirculation process covers the entire height of the enclosure as moves away from the directly exposed opening interior space. In addition, a similar temperature distribution profile having relatively weakening the influence of the incoming air plume temperature is also noticed in Figure 5(b).

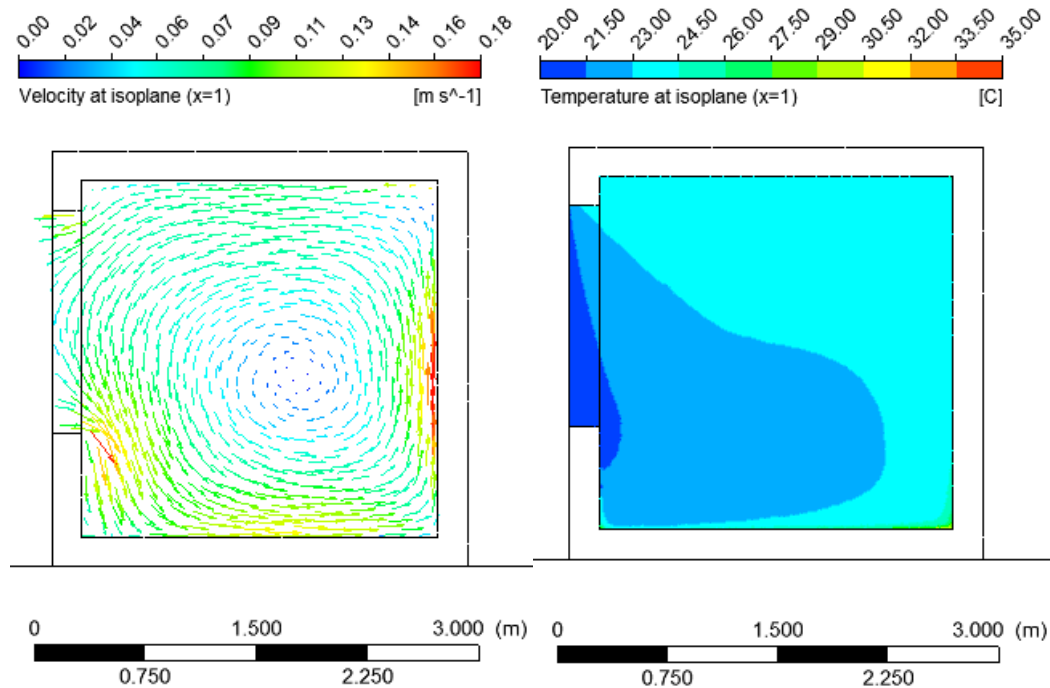


Figure 5. (a) Velocity vector (left) (b) Temperature Contour (right) at isoplane ($x = 1$)

While scrutinizing the velocity vector behavior further away from the mid-plane and close the side wall ($x=0.6$), which is not directly exposed to the opening, it is observed that the recirculation flow covers the entire height of the enclosure as presented in Figure 6 (a). However, the temperature distribution varies significantly and limited to two regions in the most part of the enclosure as seen in Figure 6 (b).

Examining the convection process further, Figure 7 (a) and (b) demonstrate the flow fields on isoplane ($y=0.6$) representing the lateral distribution close to the wall with the opening. Adding on the earlier results, it is observed in Figure 7(a) that the incoming airflow from the opening initially draws from the bottom part towards the floor with relatively higher velocity and splits into two parts creating small recirculation zones laterally on either side of the enclosure space not directly exposed to the opening. In addition, two zones of the temperature distribution demonstrating the clear influence of the outside air plume with relatively lower temperature was observed in Figure 7(b).

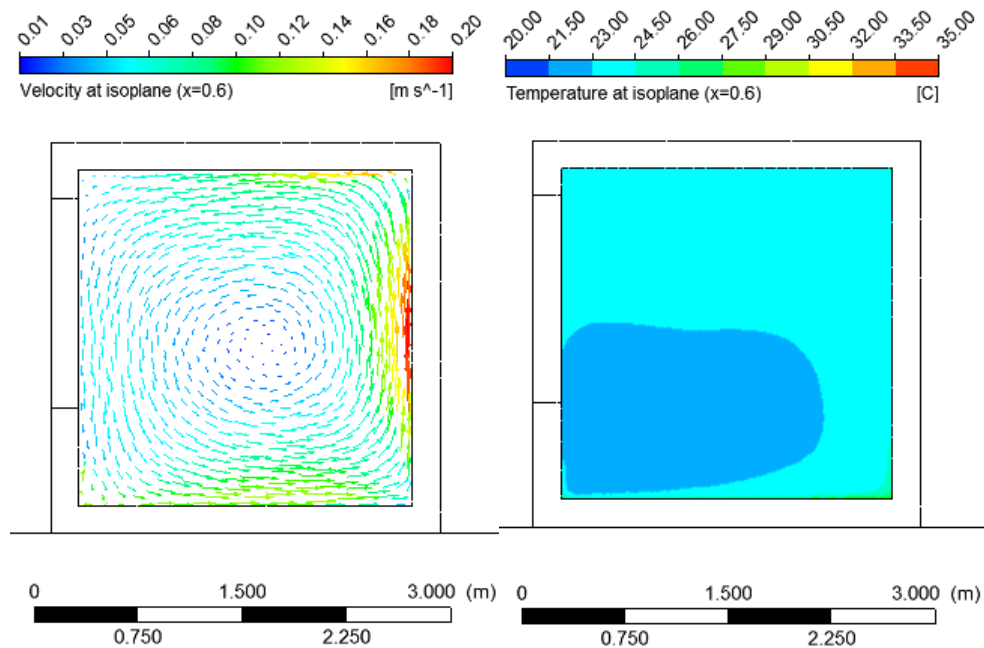


Figure 6. (a) Velocity vector (left) (b) Temperature Contour (right) at isoplane ($x = 0.6$)

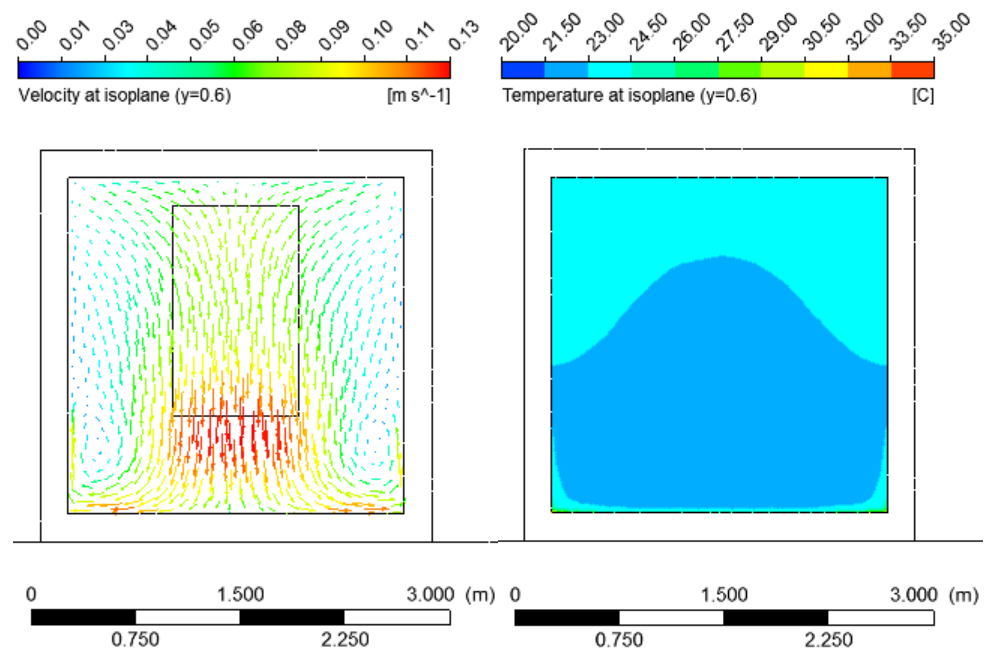


Figure 7. (a) Velocity vector (left) (b) Temperature Contour (right) at isoplane ($y = 0.6$)

Exploring it further, Figure 8 (a) and (b) demonstrate the flow fields on isoplane ($y=1.4$) representing the lateral distribution at the middle section of the enclosure. Corroborating that the intensity of the incoming flow decreases as the flow moves away from the opening, Figure 8(a) shows the similar trend of velocity vector as in Figure 7 (a), however with weak intensity. Following the similar trend of decreasing intensity as it moves away from the wall with an opening, Figure 8(b) shows the temperature distribution with reduced influence from the outdoor air temperature leading to the presence of two temperature zone.

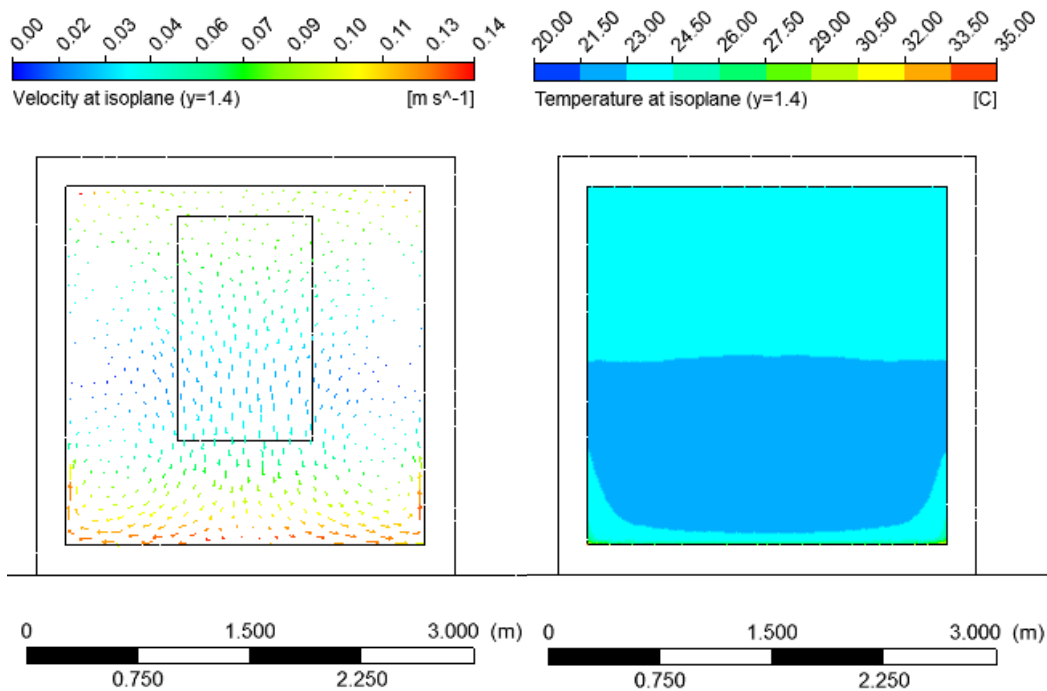


Figure 8. (a) Velocity vector (left) (b) Temperature Contour (right) at isoplane ($y = 1.4$)

Examining it further, Figure 9 (a) and (b) demonstrate the flow fields on isoplane ($y=2.2$) located farthest away from the wall with the opening. The velocity vectors observed on this plane demonstrates that the flow raises towards the roof from the floor and draws towards the top mid of the isoplane location ultimately aligning to exit to the outside environment from the top section of the opening. In addition, observing the Figure 9(b), it is obvious that the temperature distribution is more uniform on this plane as the incoming cold air plume from the opening does not directly influence it.

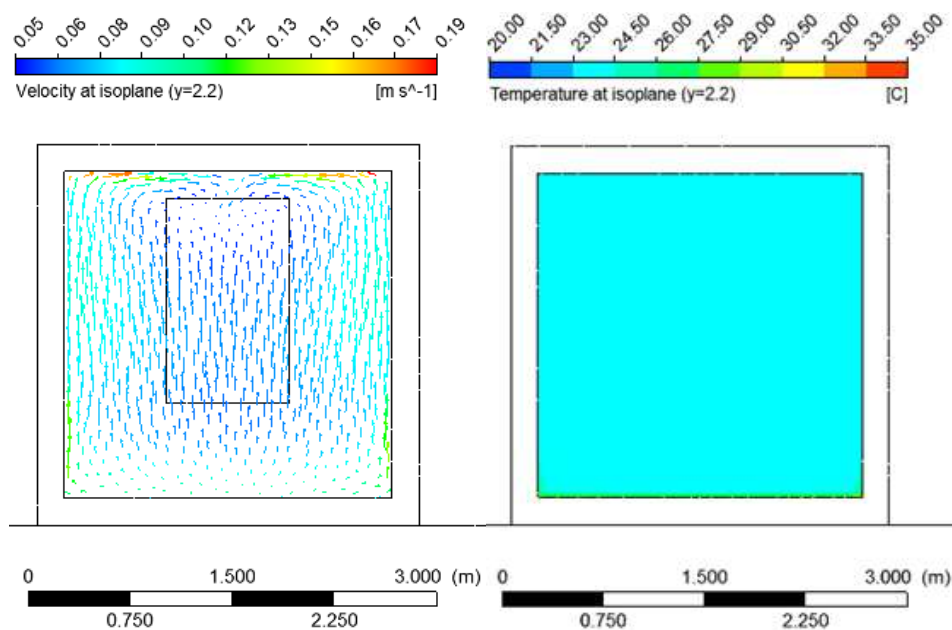


Figure 9. (a) Velocity vector (left) (b) Temperature Contour (right) at isoplane ($y = 2.2$)

Irrespective of the temperature distribution presented with maximum three different regions from Figure 4 (b) to Figure 9 (b), in reality, a very close observation with high resolution near to the floor at the mid isoplane ($x=1.4$) on Figure 10(a), reveals that a very steep graduation of decreasing temperature prevails adjacent to (within 50 mm height) the floor. In addition, besides the floor adjacent air temperature, the maximum air temperature prevails in the regions above the opening top edge throughout the enclosure, and in the region adjacent to the opposite vertical wall of the opening. Furthermore, corroborating the influence of the velocity vector pattern discussed earlier in Figure 4(a) and Figure 7(a), the spatial distribution of the heat flux decreases in both the lateral and longitudinal directions away from the initial strike core of the incoming air plume as seen in Figure 10(b).

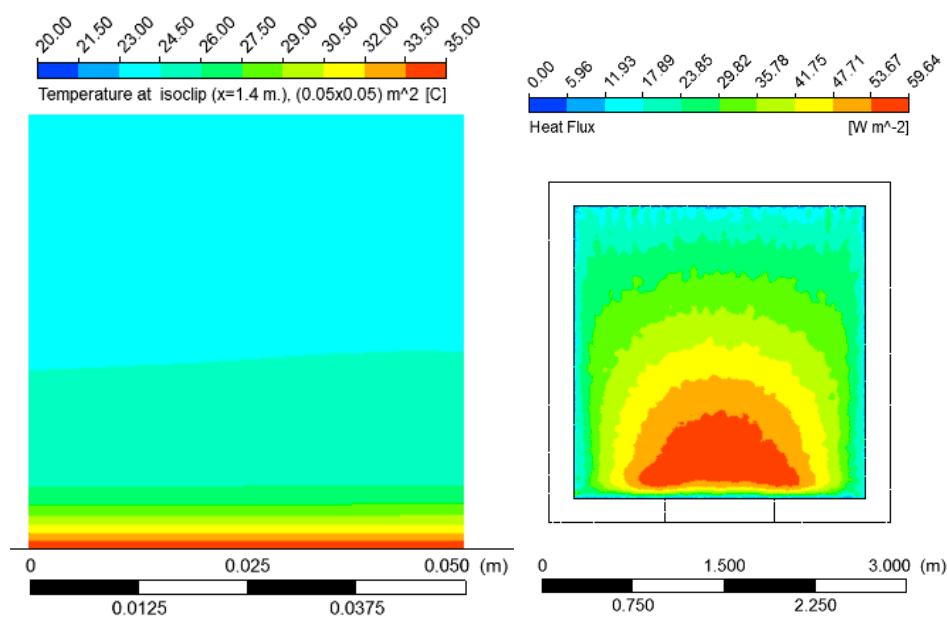


Figure 10. (a) High resolution temperature Contour ($x=1.4$) (left) (b) Spatial distribution of floor heat flux (right)

Further building on this knowledge base, Figure 11 summarizes the numerical simulations with all the 12 different cases in terms of the floor surface average Nu with respect to different values of WOF and Ra. While doing this, air properties and reference temperature were considered at the average air temperature between floor and ambient outside.

It is apparent from the results that Nu increases with Ra and WOF and this could be generalized with a correlation $Nu = 0.1593 Ra^{0.33} WOF^{0.18}$ (coefficients with 95% confidence bounds) within the ambient temperature (10°C, 15°C and 20 °C) and WOF values of (1, 0.75, 0.5 and 0.25) threshold assumed in the model. Alternatively, in terms of aspect ratio of the opening (d/D), the correlation could be expressed in the form of $Nu = 0.17 Ra^{0.33} (d/D)^{0.18}$.

A similar empirical correlation was developed by (Anderson, 2013) in the form of $Nu = 0.12 Ra^{0.34} (d/D)^{0.4}$ for $1 \times 10^8 \leq Ra \leq 5 \times 10^8$ and characteristic length of 1 m. However, a comparison of these two correlations in terms of the respective exponents of Ra indicates that overall flow regime is turbulent in nature in both studies ($n \sim 1/3$). In addition to it, a relatively higher value of coefficient term of Ra indicates that a possibility of predicting higher level of heat transfer due to a relatively higher characteristics length compared to the model and correlation of (Anderson, 2013) is enshrined in the proposed correlation.

Nevertheless, a further improvement in the proposed correlation is necessary by including the effect of the varying enclosure length, width and different height. In addition to it, possible effects due to external wind conditions, transient temperature inside the space, thermal mass of the envelope, solar gains, internal heat loads and furnishings/flow restrictions in the interior spaces also needs to be considered.

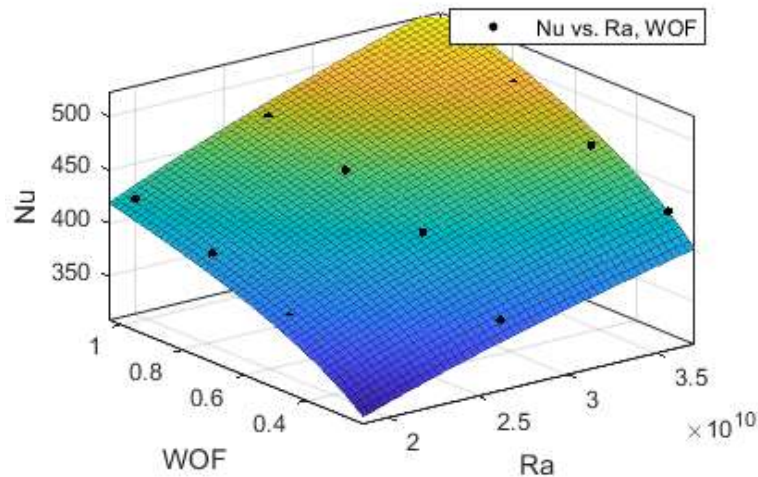


Figure 11. Average Nu with respect to WOF and Ra

4. Conclusion and Recommendation

A computational model of a single-sided partially opened 3D air filled room was examined for the variation of flow fields. Corroborating the previous studies, the work demonstrated that the heat transfer behavior of this partly open room was strongly influenced by the Ra and the WOF values. In addition to it, a significant variation in flow field were observed in 3D space resulting in a nonuniform distribution of floor heat flux on spatial context. As such, there is a significant scope of increasing the robustness of thermal models of naturally ventilated buildings by greater utilization of empirical relationships developed particularly for this purpose. Furthermore, a substantial reduction on uncertainty of estimating heat transfer seems possible by considering localized distribution of the heat flux on the floor.

Nevertheless, in reality, a naturally ventilated building is also exposed with other conditions like wind, solar gain, internal heat load, and indoor flow restrictions. It makes the problem even more complicated as these conditions might be reinforcing or restricting the airflow through the window resulting in different pattern of heat transfer behaviour. As such, a proper boundary needs to be further investigated so that the effect due to other major conditions could be integrated in the model for future refinement of the proposed correlation.

References

- Anderson, T.N. and Norris, E.S., 2016, 'Natural convection heat loss from a partly open cubic enclosure', Proceedings of the 10th Australasian Heat and Mass Transfer Conference (AHMT2016), Brisbane, Australia.
- Anderson, T. N., 2013, 'Natural convection heat transfer from a partly open enclosure', 8th Australian natural convection workshop (8ANCW), Sydney, Australia.



- Awbi, H.B. and Hatton, A., 1999, 'Natural convection from heated room surfaces', *Energy and Buildings*, 30, p233–244.
- Bilgen, E. and Muftuoglu, A., 2008, 'Natural convection in an open square cavity with slots', *International Communications in Heat and Mass Transfer*, 35, p896-900.
- Corcione, M., 2003, 'Effects of the thermal boundary conditions at the sidewalls upon natural convection in rectangular enclosures heated from below and cooled from above', *International Journal of Thermal Science*, 42, p199-208.
- Goethals, K., Breesch, H. and Janssens, Al, 2011, 'Sensitivity analysis of predicted night cooling performance to internal convective heat transfer modelling', *Energy and Building*, 43, p2429-2441.
- Hiller M., Holst, S., Welfonder, T., Weber, A., and Koschenz, M., 2002, '*TRNFLOW: Integration of the airflow model COMIS into the multi-zone building model of TRNSYS*', TRANSSOLAR Energietechnik GmbH.
- Lomas, K.J., 1996, 'The U.K. applicability study: an evaluation of thermal simulation programs for passive solar house design', *Building and Environment*, 31(3), p197-206.
- Mirsadeghi, M., Costola, D., Blocken, B. and Hensen, J.L.M., 2013, 'Review of external convective heat transfer coefficient models in building energy simulation programs: Implementation and uncertainty', *Applied Thermal Engineering*, 56, p134-151.
- Norris, E.S., Anderson, T., 2015, 'A CFD Model of Natural Convection in a Partially Open Enclosure', 9th Australasian Heat and Mass Transfer Conference (AHMT2015), Melbourne, Australia.
- Omri, M. and Galanis, N., 2007, 'Numerical analysis of turbulent buoyant flows in enclosures: Influence of grid and boundary conditions', *International Journal of Thermal Science*, 46, p727-738.
- Prakash, M., Kedare, S.B. and Nayak, J.K., 2012, 'Numerical study of natural convection loss from open cavities', *International Journal of Thermal Sciences*, 51, p23-30.
- Pokhrel, M.K., Anderson, T.N., Currie, J. and Lie, T., 2016, 'Examining the Thermal Comfort Characteristics of Naturally Ventilated Residential Buildings in New Zealand', Asia Pacific Solar Research Conference.
- Rincón-Casado, A., Sánchez de la Flor, F.J., Chacón Vera, E. and Sánchez Ramos, J., 2017, 'New natural convection heat transfer correlations in enclosures for building performance simulation', *Engineering applications of computational fluid mechanics*, 11 (1), p340-356.
- Stabat, P., Caciolo, M. and Marchio, D., 2012, 'Progress on single-sided ventilation techniques for buildings', *Advances in Building Energy Research*, 6 (2), p212-241.
- Yunus, A.C. and Afshin, J.G., 2015, 'Heat and Mass Transfer: Fundamentals and Applications, Fifth Edition, Mc-Graw Hill Education.

Acknowledgements

The authors would like to thank Callaghan Innovation, NZ for supporting project funding.